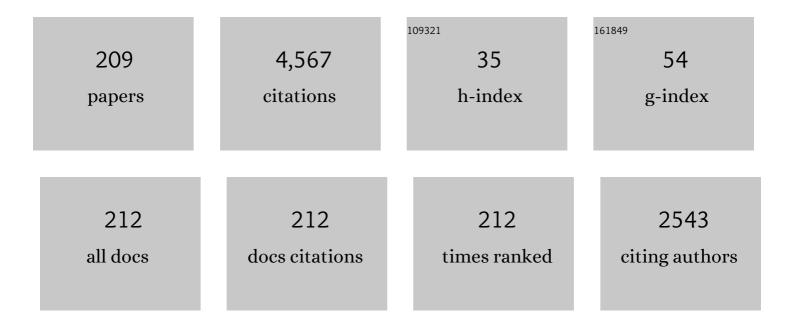
## **Dimitrios Maroudas**

List of Publications by Year in descending order

Source: https://exaly.com/author-pdf/2058794/publications.pdf Version: 2024-02-01



#	Article	IF	CITATIONS
1	Mechanism of hydrogen-induced crystallization of amorphous silicon. Nature, 2002, 418, 62-65.	27.8	379
2	"Coarse―stability and bifurcation analysis using stochastic simulators: Kinetic Monte Carlo examples. Journal of Chemical Physics, 2002, 116, 10083-10091.	3.0	113
3	Theoretical analysis of electromigration-induced failure of metallic thin films due to transgranular void propagation. Journal of Applied Physics, 1999, 85, 2233-2246.	2.5	105
4	Coarse bifurcation analysis of kinetic Monte Carlo simulations: A lattice-gas model with lateral interactions. Journal of Chemical Physics, 2002, 117, 8229-8240.	3.0	92
5	Large-scale atomistic simulations of low-energy helium implantation into tungsten single crystals. Acta Materialia, 2018, 144, 561-578.	7.9	89
6	Dynamics of small mobile helium clusters near tungsten surfaces. Surface Science, 2014, 626, L21-L25.	1.9	73
7	Absolute densities of N and excited N2 in a N2 plasma. Applied Physics Letters, 2003, 83, 4918-4920.	3.3	70
8	Opening and tuning of band gap by the formation of diamond superlattices in twisted bilayer graphene. Physical Review B, 2012, 86, .	3.2	68
9	Interactions of mobile helium clusters with surfaces and grain boundaries of plasma-exposed tungsten. Journal of Applied Physics, 2014, 115, .	2.5	66
10	Mechanical behavior of interlayer-bonded nanostructures obtained from bilayer graphene. Carbon, 2015, 81, 663-677.	10.3	64
11	Atomistic simulation study of the interactions of SiH3 radicals with silicon surfaces. Journal of Applied Physics, 1999, 86, 2872-2888.	2.5	63
12	Abstraction of hydrogen by SiH3 from hydrogen-terminated Si(001)-(2×1) surfaces. Surface Science, 1998, 418, L8-L13.	1.9	62
13	Multiscale modeling of hard materials: Challenges and opportunities for chemical engineering. AICHE Journal, 2000, 46, 878-882.	3.6	61
14	Interactions of SiH radicals with silicon surfaces: An atomic-scale simulation study. Journal of Applied Physics, 1998, 84, 3895-3911.	2.5	60
15	Electromigration-induced failure of metallic thin films due to transgranular void propagation. Applied Physics Letters, 1998, 72, 3452-3454.	3.3	59
16	Mechanical properties of irradiated single-layer graphene. Applied Physics Letters, 2013, 103, 013102.	3.3	59
17	On the origin of â€~fuzz' formation in plasma-facing materials. Nuclear Fusion, 2019, 59, 086057.	3.5	56
18	Measurement of absolute radical densities in a plasma using modulated-beam line-of-sight threshold ionization mass spectrometry. Journal of Vacuum Science and Technology A: Vacuum, Surfaces and Films, 2004, 22, 71-81.	2.1	55

#	Article	IF	CITATIONS
19	Dynamics of transgranular voids in metallic thin films under electromigration conditions. Applied Physics Letters, 1995, 67, 798-800.	3.3	53
20	Title is missing!. International Journal of Fracture, 2001, 109, 47-68.	2.2	52
21	Evolution of structure, morphology, and reactivity of hydrogenated amorphous silicon film surfaces grown by molecular-dynamics simulation. Applied Physics Letters, 2001, 78, 2685-2687.	3.3	47
22	Abstraction of atomic hydrogen by atomic deuterium from an amorphous hydrogenated silicon surface. Journal of Chemical Physics, 2002, 117, 10805-10816.	3.0	47
23	Molecular-dynamics analysis of mobile helium cluster reactions near surfaces of plasma-exposed tungsten. Journal of Applied Physics, 2015, 118, .	2.5	47
24	A Comparison of the Elastic Properties of Graphene- and Fullerene-Reinforced Polymer Composites: The Role of Filler Morphology and Size. Scientific Reports, 2016, 6, 31735.	3.3	46
25	Evidence for reduced charge recombination in carbon nanotube/perovskite-based active layers. Chemical Physics Letters, 2016, 662, 35-41.	2.6	43
26	Current-Induced Stabilization of Surface Morphology in Stressed Solids. Physical Review Letters, 2008, 100, 036106.	7.8	42
27	Elastic properties of graphene nanomeshes. Applied Physics Letters, 2014, 104, .	3.3	42
28	Theoretical study of the energetics, strain fields, and semicoherent interface structures in layer-by-layer semiconductor heteroepitaxy. Journal of Applied Physics, 1999, 85, 3677-3695.	2.5	41
29	Superlattices of Fluorinated Interlayer-Bonded Domains in Twisted Bilayer Graphene. Journal of Physical Chemistry C, 2013, 117, 7315-7325.	3.1	41
30	Helium segregation on surfaces of plasma-exposed tungsten. Journal of Physics Condensed Matter, 2016, 28, 064004.	1.8	40
31	Hydrogen-induced crystallization of amorphous silicon thin films. I. Simulation and analysis of film postgrowth treatment with H2 plasmas. Journal of Applied Physics, 2006, 100, 053514.	2.5	38
32	Tunable mechanical properties of diamond superlattices generated by interlayer bonding in twisted bilayer graphene. Applied Physics Letters, 2013, 103, .	3.3	38
33	Helium impurity transport on grain boundaries: Enhanced or inhibited?. Europhysics Letters, 2015, 110, 52002.	2.0	38
34	Helium flux effects on bubble growth and surface morphology in plasma-facing tungsten from large-scale molecular dynamics simulations. Nuclear Fusion, 2019, 59, 066035.	3.5	37
35	Modeling of radical-surface interactions in the plasma-enhanced chemical vapor deposition of silicon thin films. Advances in Chemical Engineering, 2001, 28, 251-296.	0.9	36
36	Formation of fullerene superlattices by interlayer bonding in twisted bilayer graphene. Journal of Applied Physics, 2012, 111, .	2.5	35

#	Article	IF	CITATIONS
37	Thermal conductivity of tungsten: Effects of plasma-related structural defects from molecular-dynamics simulations. Applied Physics Letters, 2017, 111, .	3.3	35
38	Theoretical Model of Helium Bubble Growth and Density in Plasma-Facing Metals. Scientific Reports, 2020, 10, 2192.	3.3	34
39	Non-linear analysis of the morphological evolution of void surfaces in metallic thin films under surface electromigration conditions. Surface Science, 1998, 415, L1055-L1060.	1.9	33
40	Mechanism and energetics of dissociative adsorption of SiH3 on the hydrogen-terminated Si(001)-(2×1) surface. Chemical Physics Letters, 2000, 329, 304-310.	2.6	33
41	Controlling assembly of colloidal particles into structured objects: Basic strategy and a case study. Journal of Process Control, 2015, 27, 64-75.	3.3	33
42	Formation and Mechanical Behavior of Nanocomposite Superstructures from Interlayer Bonding in Twisted Bilayer Graphene. ACS Applied Materials & Interfaces, 2018, 10, 28898-28908.	8.0	33
43	Effects of mechanical stress on electromigration-driven transgranular void dynamics in passivated metallic thin films. Applied Physics Letters, 1998, 73, 3848-3850.	3.3	32
44	Electromigration-driven motion of morphologically stable voids in metallic thin films: Universal scaling of migration speed with void size. Applied Physics Letters, 2004, 85, 2214-2216.	3.3	32
45	Thermally activated mechanisms of hydrogen abstraction by growth precursors during plasma deposition of silicon thin films. Journal of Chemical Physics, 2005, 122, 054703.	3.0	32
46	Theoretical study of the interactions of SiH2 radicals with silicon surfaces. Journal of Applied Physics, 1999, 86, 5497-5508.	2.5	31
47	Surface morphological response of crystalline solids to mechanical stresses and electric fields. Surface Science Reports, 2011, 66, 299-346.	7.2	31
48	Hydrogen-induced crystallization of amorphous Si thin films. II. Mechanisms and energetics of hydrogen insertion into Si–Si bonds. Journal of Applied Physics, 2006, 100, 053515.	2.5	29
49	Structure of chemisorbed acetylene on the Si(001)-(2 × 1) surface and the effect of coadsorbed atomic hydrogen. Chemical Physics Letters, 1997, 278, 97-101.	2.6	28
50	Mechanical behavior and fracture of graphene nanomeshes. Journal of Applied Physics, 2015, 117, .	2.5	28
51	Current-induced non-linear dynamics of voids in metallic thin films: morphological transition and surface wave propagation. Surface Science, 2000, 461, L550-L556.	1.9	27
52	Mechanism and activation energy barrier for H abstraction by H(D) from a-Si:H surfaces. Surface Science, 2002, 515, L469-L474.	1.9	27
53	COARSE BIFURCATION DIAGRAMS VIA MICROSCOPIC SIMULATORS: A STATE-FEEDBACK CONTROL-BASED APPROACH. International Journal of Bifurcation and Chaos in Applied Sciences and Engineering, 2004, 14, 207-220.	1.7	27
54	Semicoherent interface formation and structure in InAs/GaAs(111)A heteroepitaxy. Surface Science, 1998. 418. L68-L72.	1.9	26

#	Article	IF	CITATIONS
55	Molecular-dynamics study of the mechanism and kinetics of void growth in ductile metallic thin films. Applied Physics Letters, 2000, 77, 343-345.	3.3	26
56	Atomistic calculation of the SiH3 surface reactivity during plasma deposition of amorphous silicon thin films. Surface Science, 2004, 572, L339-L347.	1.9	26
57	Molecular-dynamics simulations of stacking-fault-induced dislocation annihilation in prestrained ultrathin single-crystalline copper films. Journal of Applied Physics, 2009, 105, .	2.5	26
58	Kinetics of strain relaxation through misfit dislocation formation in the growth of epitaxial films on compliant substrates. Applied Physics Letters, 1998, 73, 753-755.	3.3	25
59	Effects of hydrogen chemisorption on the structure and deformation of single-walled carbon nanotubes. Applied Physics Letters, 2009, 94, .	3.3	25
60	Surface Smoothening Mechanism of Amorphous Silicon Thin Films. Physical Review Letters, 2005, 95, 216102.	7.8	24
61	A Smoluchowski model of crystallization dynamics of small colloidal clusters. Journal of Chemical Physics, 2011, 135, 154506.	3.0	23
62	Thermal transport properties of graphene nanomeshes. Journal of Applied Physics, 2014, 116, 184304.	2.5	23
63	Analysis of vacancy-induced amorphization of single-layer graphene. Applied Physics Letters, 2012, 100, 203105.	3.3	22
64	Colloidal cluster crystallization dynamics. Journal of Chemical Physics, 2012, 137, 134901.	3.0	22
65	Helium segregation and transport behavior near ⟨100⟩ and ⟨110⟩ symmetric tilt grain boundaries in tungsten. Journal of Applied Physics, 2018, 123, .	2.5	22
66	Growth and characterization of hydrogenated amorphous silicon thin films from SiH2 radical precursor: Atomic-scale analysis. Journal of Applied Physics, 2004, 95, 1792-1805.	2.5	21
67	Current-driven interactions between voids in metallic interconnect lines and their effects on line electrical resistance. Applied Physics Letters, 2006, 88, 221905.	3.3	21
68	Atomic-scale analysis of defect dynamics and strain relaxation mechanisms in biaxially strained ultrathin films of face-centered cubic metals. Journal of Applied Physics, 2008, 103, .	2.5	21
69	On the hydrogen storage capacity of carbon nanotube bundles. Applied Physics Letters, 2009, 95, 163111.	3.3	21
70	Hydrogen in Si–Si bond center and platelet-like defect configurations in amorphous hydrogenated silicon. Journal of Vacuum Science & Technology an Official Journal of the American Vacuum Society B, Microelectronics Processing and Phenomena, 2004, 22, 2719.	1.6	20
71	Interaction of SiH3 radicals with deuterated (hydrogenated) amorphous silicon surfaces. Surface Science, 2005, 598, 35-44.	1.9	20
72	First-principles theoretical analysis of silyl radical diffusion on silicon surfaces. Journal of Chemical Physics, 2006, 125, 104702.	3.0	20

#	Article	IF	CITATIONS
73	Benchmarks and Tests of a Multidimensional Cluster Dynamics Model of Helium Implantation in Tungsten. Fusion Science and Technology, 2017, 71, 84-92.	1.1	20
74	Elastic Properties of Plasma-Exposed Tungsten Predicted by Molecular-Dynamics Simulations. ACS Applied Materials & amp; Interfaces, 2020, 12, 22287-22297.	8.0	20
75	Title is missing!. Journal of Computer-Aided Materials Design, 1997, 4, 63-73.	0.7	19
76	Atomistic simulation of SiH interactions with silicon surfaces during deposition from silane containing plasmas. Applied Physics Letters, 1998, 72, 578-580.	3.3	19
77	Mechanisms and energetics of SiH3 adsorption on the pristine Si(001)-(2×1) surface. Chemical Physics Letters, 2001, 344, 249-255.	2.6	19
78	Atomic pattern formation at the onset of stress-induced elastic instability: Fracture versus phase change. Physical Review B, 2004, 70, .	3.2	19
79	Molecular dynamics simulations of martensitic fcc-to-hcp phase transformations in strained ultrathin metallic films. Physical Review B, 2008, 78, .	3.2	19
80	Theoretical analysis of texture effects on the surface morphological stability of metallic thin films. Applied Physics Letters, 2008, 92, 181905.	3.3	19
81	Theory of multiple quantum dot formation in strained-layer heteroepitaxy. Applied Physics Letters, 2016, 109, .	3.3	19
82	Multiscale Shear-Lag Analysis of Stiffness Enhancement in Polymer–Graphene Nanocomposites. ACS Applied Materials & Interfaces, 2017, 9, 23092-23098.	8.0	19
83	Atomistic mechanisms of strain relaxation due to ductile void growth in ultrathin films of face-centered-cubic metals. Journal of Applied Physics, 2005, 97, 113527.	2.5	18
84	Effects of electromigration-induced void dynamics on the evolution of electrical resistance in metallic interconnect lines. Applied Physics Letters, 2005, 86, 241905.	3.3	18
85	Analysis of diamond nanocrystal formation from multiwalled carbon nanotubes. Physical Review B, 2009, 80, .	3.2	18
86	Kinetic Monte Carlo simulations of surface growth during plasma deposition of silicon thin films. Journal of Chemical Physics, 2009, 131, 034503.	3.0	18
87	Modeling Helium Segregation to the Surfaces of Plasma-Exposed Tungsten as a Function of Temperature and Surface Orientation. Fusion Science and Technology, 2017, 71, 22-35.	1.1	18
88	In Situ Probing and Atomistic Simulation of a-Si:H Plasma Deposition. Materials Research Society Symposia Proceedings, 2001, 664, 111.	0.1	17
89	Electromigration-induced wave propagation on surfaces of voids in metallic thin films: Hopf bifurcation for high grain symmetry. Surface Science, 2005, 575, L41-L50.	1.9	17
90	Prediction of temperature range for the onset of fuzz formation in helium-plasma-implanted tungsten. Surface Science, 2020, 698, 121614.	1.9	17

#	Article	IF	CITATIONS
91	Analysis of damage formation and propagation in metallic thin films under the action of thermal stresses and electric fields. Journal of Computer-Aided Materials Design, 1996, 2, 231-258.	0.7	16
92	Interfacial stability and misfit dislocation formation in InAs/GaAs(110) heteroepitaxy. Surface Science, 1998, 411, L865-L871.	1.9	16
93	Nonhydrostatic stress effects on failure of passivated metallic thin films due to void surface electromigration. Surface Science, 1999, 432, L604-L610.	1.9	16
94	Temperature dependence of precursor–surface interactions in plasma deposition of silicon thin films. Chemical Physics Letters, 2005, 414, 61-65.	2.6	16
95	Stress-induced deceleration of electromigration-driven void motion in metallic thin films. Journal of Applied Physics, 2007, 101, 063513.	2.5	16
96	Dynamics of Small Mobile Helium Clusters Near a Symmetric Tilt Grain Boundary of Plasma-Exposed Tungsten. Fusion Science and Technology, 2017, 71, 36-51.	1.1	16
97	Continuum and atomistic modeling of electromechanically-induced failure of ductile metallic thin films. Computational Materials Science, 2002, 23, 242-249.	3.0	15
98	Hopf bifurcation, bistability, and onset of current-induced surface wave propagation on void surfaces in metallic thin films. Surface Science, 2008, 602, 1227-1242.	1.9	15
99	Analysis of Charge Transport and Device Performance in Organic Photovoltaic Devices with Active Layers of Self-Assembled Nanospheres. Journal of Physical Chemistry C, 2015, 119, 25826-25839.	3.1	15
100	Current-driven nanowire formation on surfaces of crystalline conducting substrates. Applied Physics Letters, 2016, 108, 193109.	3.3	15
101	Surface morphology in InAs/GaAs(111)A heteroepitaxy: Experimental measurements and computer simulations. Applied Physics Letters, 1999, 75, 829-831.	3.3	14
102	Thermal activation of shear modulus instabilities in pressure-inducedbcc→hcptransitions. Physical Review B, 2000, 62, 13799-13802.	3.2	14
103	Applicability of Born's stability criterion to face-centered-cubic crystals in [111] loading. Applied Physics Letters, 2005, 87, 251919.	3.3	14
104	Rippling instability on surfaces of stressed crystalline conductors. Applied Physics Letters, 2009, 94, 181911.	3.3	14
105	Dynamics of the <mml:math <br="" xmlns:mml="http://www.w3.org/1998/Math/MathML">display="inline"&gt;<mml:mrow><mml:mtext>bcc</mml:mtext><mml:mo>→</mml:mo><mml:mtext>hcpin crystals under uniaxial stress. Physical Review B, 2009, 79, .</mml:mtext></mml:mrow></mml:math>	nte <b>st</b> 2 <td>ml<b>:114</b>row&gt;</td>	ml <b>:114</b> row>
106	Effects of surface diffusional anisotropy on the current-driven surface morphological response of stressed solids. Journal of Applied Physics, 2010, 107, 093527.	2.5	14
107	Surface nanopatterning from current-driven assembly of single-layer epitaxial islands. Applied Physics Letters, 2013, 103, .	3.3	14
108	Kinetics of strain relaxation through misfit dislocation formation in InAs/GaAs(111)A heteroepitaxy. Surface Science, 1999, 441, L911-L916.	1.9	13

#	Article	IF	CITATIONS
109	Relaxation of biaxial tensile strain in ultrathin metallic films: Ductile void growth versus nanocrystalline domain formation. Applied Physics Letters, 2005, 87, 171913.	3.3	13
110	Theoretical analysis of current-driven interactions between voids in metallic thin films. Journal of Applied Physics, 2007, 101, 023518.	2.5	13
111	Electromigration-driven surface morphological stabilization of a coherently strained epitaxial thin film on a substrate. Applied Physics Letters, 2010, 96, 231911.	3.3	13
112	Current-induced stabilization of surface morphology in stressed solids: Validation of linear stability theory. Journal of Applied Physics, 2010, 107, .	2.5	13
113	Theory of surface segregation in ternary semiconductor quantum dots. Applied Physics Letters, 2011, 98, .	3.3	13
114	Current-driven morphological evolution of single-layer epitaxial islands on crystalline substrates. Surface Science, 2013, 618, L1-L5.	1.9	13
115	Atomic-scale analysis of deposition and characterization ofa-Si:H thin films grown from SiH radical precursor. Journal of Applied Physics, 2002, 92, 842-852.	2.5	12
116	Void nucleation in biaxially strained ultrathin films of face-centered cubic metals. Applied Physics Letters, 2007, 90, 221907.	3.3	12
117	Comparative study of the mechanical behavior under biaxial strain of prestrained face-centered cubic metallic ultrathin films. Applied Physics Letters, 2009, 94, 101911.	3.3	12
118	Hydrogenation effects on the structure and morphology of graphene and single-walled carbon nanotubes. Journal of Applied Physics, 2010, 108, 113532.	2.5	12
119	Analysis of current-driven oscillatory dynamics of single-layer homoepitaxial islands on crystalline conducting substrates. Surface Science, 2018, 669, 25-33.	1.9	12
120	Mechanical behavior of thin buffer layers in InAs/GaAs(111)A heteroepitaxy. Applied Physics Letters, 2000, 76, 3017-3019.	3.3	11
121	Atomic-scale analysis of fundamental mechanisms of surface valley filling during plasma deposition of amorphous silicon thin films. Surface Science, 2005, 574, 123-143.	1.9	11
122	Surface smoothness of plasma-deposited amorphous silicon thin films: Surface diffusion of radical precursors and mechanism of Si incorporation. Physical Review B, 2006, 74, .	3.2	11
123	Stability of simple cubic crystals. Applied Physics Letters, 2007, 90, 161910.	3.3	11
124	First-principles theoretical analysis of pure and hydrogenated crystalline carbon phases and nanostructures. Chemical Physics Letters, 2009, 474, 168-174.	2.6	11
125	Phase behavior of the 38-atom Lennard-Jones cluster. Journal of Chemical Physics, 2014, 140, 104312.	3.0	11
126	Mechanical properties of hydrogenated electron-irradiated graphene. Journal of Applied Physics, 2016, 120, 124301.	2.5	11

#	Article	IF	CITATIONS
127	Effects of elastic softening and helium accumulation kinetics on surface morphological evolution of plasma-facing tungsten. Nuclear Fusion, 2021, 61, 016016.	3.5	11
128	Atomistic analysis of the mechanism of hydrogen diffusion in plasma-deposited amorphous silicon thin films. Applied Physics Letters, 2005, 87, 261911.	3.3	10
129	Interactions between radical growth precursors on plasma-deposited silicon thin-film surfaces. Journal of Chemical Physics, 2007, 126, 114704.	3.0	10
130	Analysis of current-driven surface morphological stabilization of a coherently strained epitaxial thin film on a finite-thickness deformable substrate. Journal of Applied Physics, 2010, 108, 093517.	2.5	10
131	Surface morphological stabilization of stressed crystalline solids by simultaneous action of applied electric and thermal fields. Applied Physics Letters, 2012, 100, .	3.3	10
132	Weakly nonlinear theory of secondary rippling instability in surfaces of stressed solids. Journal of Applied Physics, 2015, 118, .	2.5	10
133	Molecular dynamics study of the interactions of small thermal and energetic silicon clusters with crystalline and amorphous silicon surfaces. Journal of Vacuum Science & Technology an Official Journal of the American Vacuum Society B, Microelectronics Processing and Phenomena, 2001, 19, 634.	1.6	9
134	Thermodynamic instability of ZnSe/ZnS core/shell quantum dots. Journal of Applied Physics, 2012, 111, 113526.	2.5	9
135	Design of semiconductor ternary quantum dots with optimal optoelectronic function. AICHE Journal, 2013, 59, 3223-3236.	3.6	9
136	Stabilization of the surface morphology of stressed solids using thermal gradients. Applied Physics Letters, 2014, 104, .	3.3	9
137	Equilibrium Shape of Colloidal Crystals. Langmuir, 2015, 31, 11428-11437.	3.5	9
138	Complex Pattern Formation from Current-Driven Dynamics of Single-Layer Homoepitaxial Islands on Crystalline Conducting Substrates. Physical Review Applied, 2017, 8, .	3.8	9
139	Thermal conductivity of electron-irradiated graphene. Applied Physics Letters, 2017, 111, .	3.3	9
140	Charge transfer properties of diphenyl substituted cyclopentadithiophene organic semiconductors: The role of fluorine and malononitrile substitutions and crystal ordering. Organic Electronics, 2017, 50, 130-137.	2.6	9
141	Electronic structure of electron-irradiated graphene and effects of hydrogen passivation. Materials Research Express, 2018, 5, 115603.	1.6	9
142	Effects of pore morphology and pore edge termination on the mechanical behavior of graphene nanomeshes. Journal of Applied Physics, 2019, 126, 164306.	2.5	9
143	Molecular-Dynamics Simulations on Nanoindentation of Graphene-Diamond Composite Superstructures in Interlayer-Bonded Twisted Bilayer Graphene: Implications for Mechanical Metamaterials. ACS Applied Nano Materials, 2021, 4, 8611-8625.	5.0	9
144	Theory and Computer Simulation of Grain-Boundary and Void Dynamics in Polycrystalline Conductors. Materials Research Society Symposia Proceedings, 1995, 391, 151.	0.1	8

#	Article	IF	CITATIONS
145	Deformation behavior of coherently strained InAs/GaAs(111)A heteroepitaxial systems: Theoretical calculations and experimental measurements. Journal of Applied Physics, 2001, 90, 2689-2698.	2.5	8
146	Coarse molecular-dynamics analysis of stress-induced structural transitions in crystals. Applied Physics Letters, 2007, 90, 171910.	3.3	8
147	Current-induced surface roughness reduction in conducting thin films. Applied Physics Letters, 2017, 110, 103103.	3.3	8
148	Optimization of electrical treatment strategy for surface roughness reduction in conducting thin films. Journal of Applied Physics, 2018, 124, 125302.	2.5	8
149	Coarse molecular-dynamics determination of the onset of structural transitions: Melting of crystalline solids. Physical Review B, 2006, 74, .	3.2	7
150	First-principles theoretical analysis of sequential hydride dissociation on surfaces of silicon thin films. Applied Physics Letters, 2007, 90, 251915.	3.3	7
151	Mechanisms and energetics of hydride dissociation reactions on surfaces of plasma-deposited silicon thin films. Journal of Chemical Physics, 2007, 127, 194703.	3.0	7
152	Formation of core/shell-like ZnSe1â^'xTex nanocrystals due to equilibrium surface segregation. Applied Physics Letters, 2010, 96, .	3.3	7
153	Analysis of electromechanically induced long-wavelength rippling instability on surfaces of crystalline conductors. Journal of Applied Physics, 2011, 109, 053518.	2.5	7
154	Onset of the crystalline phase in small assemblies of colloidal particles. Applied Physics Letters, 2013, 102, .	3.3	7
155	Strain relaxation and interfacial stability in III–V semiconductor strained-layer heteroepitaxy: atomistic and continuum modeling and comparisons with experiments. Computational Materials Science, 2002, 23, 250-259.	3.0	6
156	Mechanism and energetics of dimerization of SiH2 radicals on H-terminated Si()-(2×1) surfaces. Surface Science, 2003, 540, L623-L630.	1.9	6
157	Strain Relaxation in Si1-xGex Thin Films on Si (100) Substrates: Modeling and Comparisons with Experiments. Materials Research Society Symposia Proceedings, 2005, 875, 1.	0.1	6
158	Current-induced wave propagation on surfaces of voids in metallic thin films with high symmetry of surface diffusional anisotropy. Journal of Applied Physics, 2007, 102, 073506.	2.5	6
159	Surface nanopattern formation due to current-induced homoepitaxial nanowire edge instability. Applied Physics Letters, 2016, 109, .	3.3	6
160	Tuning the band structure of graphene nanoribbons through defect-interaction-driven edge patterning. Physical Review B, 2017, 96, .	3.2	6
161	Structure-properties relations in graphene derivatives and metamaterials obtained by atomic-scale modeling. Molecular Simulation, 2019, 45, 1173-1202.	2.0	6
162	Non-dilute helium-related defect interactions in the near-surface region of plasma-exposed tungsten. Journal of Applied Physics, 2020, 128, .	2.5	6

#	Article	IF	CITATIONS
163	Molecular-Dynamics Analysis of Nanoindentation of Graphene Nanomeshes: Implications for 2D Mechanical Metamaterials. ACS Applied Nano Materials, 2020, 3, 3613-3624.	5.0	6
164	Hole formation effect on surface morphological response of plasma-facing tungsten. Journal of Applied Physics, 2021, 129, 193302.	2.5	6
165	Onset of fuzz formation in plasma-facing tungsten as a surface morphological instability. Physical Review Materials, 2021, 5, .	2.4	6
166	Analysis of elastic stability and structural response of face-centered cubic crystals subject to [110] loading. Applied Physics Letters, 2006, 89, 181907.	3.3	5
167	Coarse molecular-dynamics analysis of an order-to-disorder transformation of a krypton monolayer on graphite. Journal of Chemical Physics, 2008, 129, 184106.	3.0	5
168	Mechanical behavior of ultralow-dielectric-constant mesoporous amorphous silica. Applied Physics Letters, 2008, 92, 251903.	3.3	5
169	Equilibrium compositional distribution in freestanding ternary semiconductor quantum dots: The case of InxGa1â <sup>°°</sup> xAs. Journal of Chemical Physics, 2011, 135, 234701.	3.0	5
170	Compositional effects on the electronic structure of ZnSe1â^'xSx ternary quantum dots. Applied Physics Letters, 2011, 99, .	3.3	5
171	The effect of a compliant substrate on the electromigration-driven surface morphological stabilization of an epitaxial thin film. Journal of Applied Physics, 2012, 111, 024905.	2.5	5
172	Stabilization of the surface morphology of stressed solids using simultaneously applied electric fields and thermal gradients. Journal of Applied Physics, 2014, 116, .	2.5	5
173	Interfacial stability and structure in InAs/GaAs(111)A heteroepitaxy: Effects of buffer layer thickness and film compositional grading. Applied Physics Letters, 2000, 77, 3352-3354.	3.3	4
174	Effects of buffer layer thickness and film compositional grading on strain relaxation kinetics in InAs/GaAs(111)A heteroepitaxy. Surface Science, 2000, 463, L634-L640.	1.9	4
175	On the growth mechanism of plasma deposited amorphous silicon thin films. Applied Physics Letters, 2008, 93, 151913.	3.3	4
176	Electromechanically driven chaotic dynamics of voids in metallic thin films. Physical Review B, 2010, 81, .	3.2	4
177	Analysis of current-driven motion of morphologically stable voids in metallic thin films: Steady and time-periodic states. Journal of Applied Physics, 2010, 108, 053514.	2.5	4
178	Mechanical properties of ultralow-dielectric-constant mesoporous amorphous silica structures: Effects of pore morphology and loading mode. Applied Physics Letters, 2011, 98, .	3.3	4
179	The effect of a thermal gradient on the electromigration-driven surface morphological stabilization of an epitaxial thin film on a compliant substrate. Journal of Applied Physics, 2013, 114, 023503.	2.5	4
180	Theoretical design of new cyclopentadithiophene-based organic semiconductors with tunable nature and performance. Synthetic Metals, 2019, 258, 116196.	3.9	4

#	Article	IF	CITATIONS
181	Design of semiconductor surface pits for fabrication of regular arrays of quantum dots and nanorings. Journal of Applied Physics, 2019, 125, .	2.5	4
182	Kinetics of nanoring formation on surfaces of stressed thin films. Physical Review Materials, 2018, 2, .	2.4	4
183	First-principles theoretical analysis of dopant adsorption and diffusion on surfaces of ZnSe nanocrystals. Chemical Physics Letters, 2008, 462, 265-268.	2.6	3
184	Effects of composition and compositional distribution on the electronic structure of ZnSe1â^'xTex ternary quantum dots. Journal of Applied Physics, 2011, 110, 123509.	2.5	3
185	Kinetics of interdiffusion in semiconductor ternary quantum dots. Applied Physics Letters, 2012, 101, .	3.3	3
186	Tunable Percolation in Semiconducting Binary Polymer Nanoparticle Glasses. Journal of Physical Chemistry B, 2016, 120, 2544-2556.	2.6	3
187	Modeling of quantum dot and nanoring pattern formation on pit-patterned semiconductor substrates. Materials Research Express, 2018, 5, 086303.	1.6	3
188	On the formation of multiple quantum dots inside elongated pits on semiconductor films deposited epitaxially on pit-patterned substrates. Materials Research Express, 2019, 6, 086328.	1.6	3
189	Atomic-scale modeling toward enabling models of surface nanostructure formation in plasma-facing materials. Current Opinion in Chemical Engineering, 2019, 23, 77-84.	7.8	3
190	Fabrication of Ordered Arrays of Quantum Dot Molecules Based on the Design of Pyramidal Pit Patterns on Semiconductor Surfaces. Industrial & Engineering Chemistry Research, 2020, 59, 2536-2547.	3.7	3
191	Atomic-Scale Analysis of the Reactivity of Radicals from Silane/Hydrogen Plasmas with Silicon Surfaces. Materials Research Society Symposia Proceedings, 1997, 485, 107.	0.1	2
192	Theoretical Analysis of Faceted Void Dynamics in Metallic Thin Films Under Electromigration Conditions. Materials Research Society Symposia Proceedings, 1998, 529, 21.	0.1	2
193	Combined effects of substrate compliance and film compositional grading on strain relaxation in layer-by-layer semiconductor heteroepitaxy: the case of InAs/In0.50Ga0.50As/GaAs(111)A. Surface Science, 2003, 540, 363-378.	1.9	2
194	Atomistic analysis of strain relaxation in [11Â <sup>-</sup> 0]-oriented biaxially strained ultrathin copper films. Journal of Applied Physics, 2009, 106, 103519.	2.5	2
195	Effect of helium flux on near-surface helium accumulation in plasma-exposed tungsten. Journal of Physics Condensed Matter, 2022, 34, 035701.	1.8	2
196	Thermal gradient effect on helium and self-interstitial transport in tungsten. Journal of Applied Physics, 2021, 130, .	2.5	2
197	Theoretical Analysis of Electromigration-Induced Failure of Metallic Thin Films. Materials Research Society Symposia Proceedings, 1997, 505, 249.	0.1	1
198	Atomic-Scale Analysis of Plasma-Enhanced Chemical Vapor Deposition from SiH4/2 Plasmas on Si Substrates. Materials Research Society Symposia Proceedings, 1998, 507, 673.	0.1	1

#	Article	IF	CITATIONS
199	Analysis of Failure in Metallic Thin-Film Interconnects Due to Stress and Electromigration-Induced Void Propagation. Materials Research Society Symposia Proceedings, 1998, 516, 165.	0.1	1
200	Surface Processes during Growth of Hydrogenated Amorphous Silicon. Materials Research Society Symposia Proceedings, 2004, 808, 311.	0.1	1
201	Effect of applied stress tensor anisotropy on the electromechanically driven complex dynamics of void surfaces in metallic thin films. Journal of Applied Physics, 2011, 110, .	2.5	1
202	Electromigration-driven complex dynamics of void surfaces in stressed metallic thin films under a general biaxial mechanical loading. Journal of Applied Physics, 2012, 112, 083523.	2.5	1
203	Strain Effects on the Diffusion Properties of Near-Surface Self-Interstitial Atoms and Adatoms in Tungsten. Frontiers in Materials, 2021, 8, .	2.4	1
204	Interfacial Stability and Surface Morphology in Layer-By-Layer Semiconductor Heteroepitaxy Luis. Materials Research Society Symposia Proceedings, 1998, 528, 153.	0.1	0
205	Analysis of Electromigration- and Stress-Induced Dynamical Response of Voids Confined in Metallic Thin Films. Materials Research Society Symposia Proceedings, 2005, 899, 1.	0.1	0
206	Atomic-Scale Analysis of Strain Relaxation Mechanisms in Ultra-Thin Metallic Films. Materials Research Society Symposia Proceedings, 2005, 880, 1.	0.1	0
207	The Role of SiH3 Diffusion in Determining the Surface Smoothness of Plasma-Deposited Amorphous Si Thin Films: An Atomic-Scale Analysis. Materials Research Society Symposia Proceedings, 2005, 862, 321.	0.1	0
208	Analysis of Electromigration-Induced Void Motion and Surface Oscillations in Metallic Thin-Film Interconnects. Materials Research Society Symposia Proceedings, 2005, 863, B9.8-1.	0.1	0
209	Effects of the Attractive Potential Range on the Phase Behavior of Small Clusters of Colloidal Particles. Journal of Chemical & Engineering Data, 2014, 59, 3105-3112.	1.9	Ο